

Article

County-Based PM_{2.5} Concentrations' Prediction and Its Relationship with Urban Landscape Pattern

Lijuan Yang ¹, Shuai Wang ¹, Xiujuan Hu ² and Tingting Shi ^{3,*} ¹ College of Geography and Oceanography, Minjiang University, Fuzhou 350118, China² College of Environment and Safety Engineering, Fuzhou University, Fuzhou 350108, China³ School of Economics and Management, Minjiang University, Fuzhou 350108, China

* Correspondence: shitingting@mju.edu.cn

Abstract: Satellite top-of-atmosphere (TOA) reflectance has been validated as an effective index for estimating PM_{2.5} concentrations due to its high spatial coverage and relatively high spatial resolution (i.e., 1 km). For this paper, we developed an ensemble random forest (RF) model incorporating satellite top-of-atmosphere (TOA) reflectance with four categories of supplemental parameters to derive the PM_{2.5} concentrations in the region of the Yangtze River Delta-Fujian (i.e., YRD-FJ) located in east China. The landscape pattern indices at two levels (i.e., type level and overall level) retrieved from 3-year land classification imageries (i.e., 2016, 2018, and 2020) were used to discuss the correlation between county-based PM_{2.5} values and landscape pattern. We achieved a cross validation R² of 0.91 (RMSE = 9.06 µg/m³), 0.89 (RMSE = 10.19 µg/m³), and 0.90 (RMSE = 8.02 µg/m³) between the estimated and observed PM_{2.5} concentrations in 2016, 2018, and 2020, respectively. The PM_{2.5} distribution retrieved from the RF model showed a trend of a year-on-year decrease with the pattern of “Jiangsu > Shanghai > Zhejiang > Fujian” in the YRD-FJ region. Our results also revealed that the landscape pattern of farmland, water bodies, and construction land exhibited a highly positive relationship with the county-based average PM_{2.5} values, as the *r* coefficients reached 0.74 while the forest land was negatively correlated with the county-based PM_{2.5} (*r* = 0.84). There was also a significant correlation between the county-based PM_{2.5} and shrubs (*r* = 0.53), grass land (*r* = 0.76), and bare land (*r* = 0.60) in the YRD-FJ region, respectively. Three landscape pattern indices at an overall level were positively correlated with county-based PM_{2.5} concentrations (*r* = 0.80), indicating that the large landscape fragmentation, edge density, and landscape diversity would raise the PM_{2.5} pollution in the study region.

Keywords: random forest; PM_{2.5}; landscape pattern; YRD-FJ

Citation: Yang, L.; Wang, S.; Hu, X.; Shi, T. County-Based PM_{2.5} Concentrations' Prediction and Its Relationship with Urban Landscape Pattern. *Processes* **2023**, *11*, 704. <https://doi.org/10.3390/pr11030704>

Academic Editors: Mohammed Mahbubul Islam and Md Azhar

Received: 30 January 2023
Revised: 14 February 2023
Accepted: 16 February 2023
Published: 26 February 2023



Copyright: © 2023 by the authors. Licensee MDPI, Basel, Switzerland. This article is an open access article distributed under the terms and conditions of the Creative Commons Attribution (CC BY) license (<https://creativecommons.org/licenses/by/4.0/>).

1. Introduction

Air pollution has become one of the most important environmental problems over the urban regions in China. Studies have shown that fine particulate matter suspended in the air (i.e., PM_{2.5}) not only has a seriously negative impact on the ecological environment but is also significantly associated with human health [1–3]. PM_{2.5} has been reported to be one of the primary pollutants that affect the air quality in major cities of mainland China [4,5]. A large amount of remote sensing data has provided an effective means for retrieving PM_{2.5} distribution [6–8].

The remote sensing data sets that have been widely used for regional PM_{2.5} estimation are the aerosol optical depth (AOD) products from various sensors with different spatial resolutions (1–17.6 km), and the methods for PM_{2.5} estimation based on AOD data have evolved from simple linear models [9,10] to advanced statistical models [11,12] and machine learning [13–15]. Compared with simple linear models, these two more complex methods have introduced a large number of auxiliary factors (e.g., meteorological parameters, road density, population density, and land use parameters) that directly or indirectly affect the

regional PM_{2.5} concentrations; therefore, the accuracy of the model's estimation has been much improved over linear models. For example, Ma et al. [16] used the linear mixed effects model incorporating meteorological parameters and land use information, and their results showed that the model's predictability was significantly improved. He and Huang [17] established a geographically and temporally weighted regression (GTWR) model by using AOD and seven parameters for estimating PM_{2.5} in China, and they achieved an R^2 of 0.80.

In addition to the AOD products, the satellite top-of-atmosphere (TOA) reflectance at the blue, red, and mid-infrared bands that are used to retrieve the AOD distribution has also been demonstrated to be an effective variable for retrieving the PM_{2.5} values [18,19]. For example, Shen proposed a deep belief network model for PM_{2.5} estimation in Wuhan by using satellite TOA reflectance and obtained an R^2 of 0.87 for the model's performance. Yang and Shi [18] successfully obtained the PM_{2.5} concentrations using TOA reflectance in east China, and the cross-validated R^2 reached 0.87. These studies demonstrated that the satellite TOA reflectance combined with meteorological fields and other auxiliary parameters can be used to estimate the regional PM_{2.5} concentrations.

Both the abovementioned complex methods showed significantly high performance in estimating PM_{2.5} concentrations with full coverage over the urban regions. Discussions of the correlation of fully-covered PM_{2.5} concentrations and regional population distribution were then carried out to study the risk of PM_{2.5} population exposure [20,21]. McCarty and Kaza [22] revealed that the land use types and urban landscape patterns would also affect the spatial distribution of regional PM_{2.5} concentrations; e.g., the area of the forest land was significantly negatively correlated with fine particulate matters while the construction land showed a highly positive relationship with PM_{2.5} concentrations. However, there is no clear conclusion reported for the relationship of PM_{2.5} concentrations and other land use types (e.g., water bodies and shrubs). Currently, most of the studies obtained the urban landscape metrics by using a moving window method or establishing a buffer zone with different radiuses centered on the monitoring stations to discuss the PM_{2.5}–landscape pattern relationship [23,24]; the research focusing on county-scale PM_{2.5} concentrations and the urban landscape pattern is still limited. Therefore, for this paper, a random forest (RF) method using TOA reflectance and four categories of supplemental parameters was first developed for estimating the PM_{2.5} concentrations in the contiguous Yangtze River Delta and Fujian Province (i.e., YRD-FJ) located in east China. Three land classification imageries (i.e., 2016, 2018, and 2020) with a spatial resolution of 30 m were then employed for retrieving the urban landscape metrics based on 285 counties of the YRD-FJ region. Finally, the correlation of a county-based PM_{2.5} distribution and urban landscape pattern at two levels (i.e., type level and overall level) was discussed so as to provide a scientific support for improving the ecological environment in the YRD-FJ region.

2. Study Area and Methods

2.1. Study Area

We defined the contiguous Yangtze River Delta and Fujian Province (i.e., YRD-FJ) located in east China as the study area where the YRD region contains three provinces/municipalities, i.e., Jiangsu Province (95 counties), Zhejiang Province (90 counties), and Shanghai (16 counties), and Fujian Province has a total of 84 counties (Figure 1). The YRD region, adjacent to the Yellow Sea and the East China Sea, is one of the most economically developed regions in China, with an urbanization rate of over 60% and a total economic volume of 25% of China's GDP by the end of 2020. With rapid economic development, the air quality has deteriorated in the YRD region with PM_{2.5} concentrations higher than 50 $\mu\text{g}/\text{m}^3$ over the last decade. Fujian Province, bordered by Zhejiang Province in the north, is dominated by mountains and hills with a forest coverage rate of 66.8%, which makes the air quality much better than most of the regions in China.

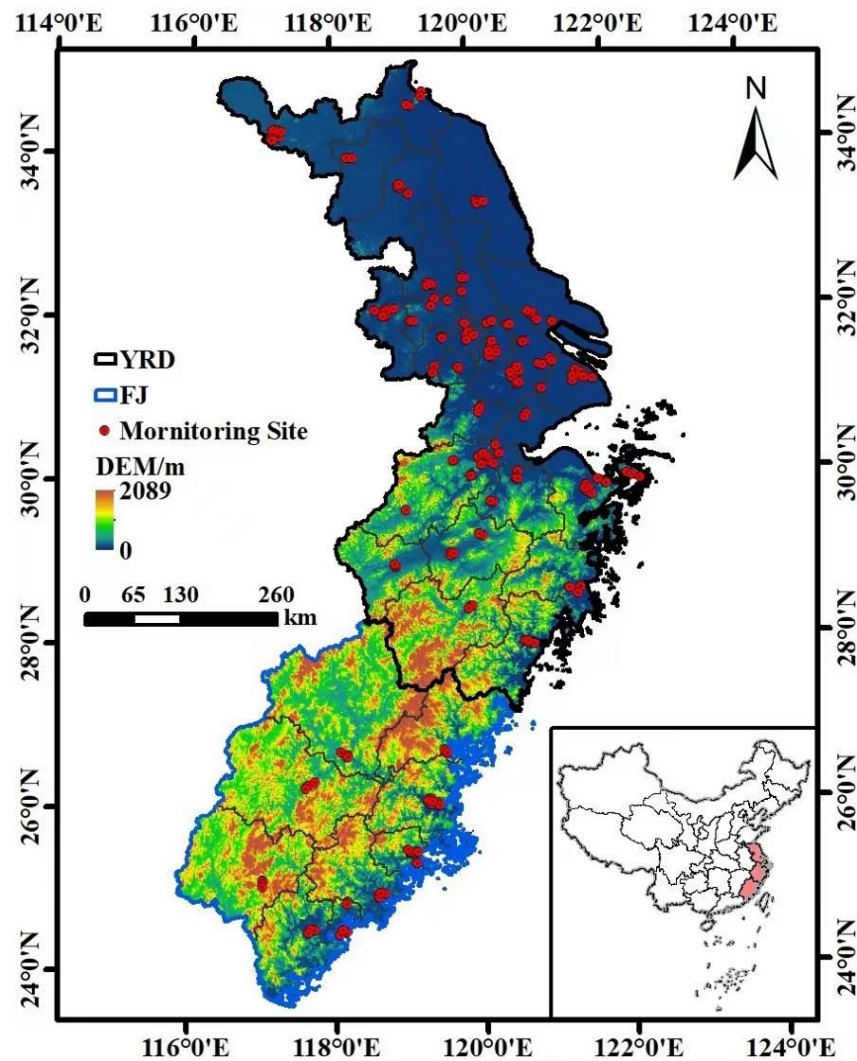


Figure 1. The study area (YRD-FJ).

2.2. Modeling Data Materials

2.2.1. In Situ $PM_{2.5}$

The $PM_{2.5}$ was obtained from a total of 195 environmental monitoring stations monitored by the Environmental Protection Departments of Jiangsu, Zhejiang, Fujian, and Shanghai from 1 January 2016 to 31 December 2020. Anomalous values with $PM_{2.5}$ concentrations less than zero and recorded as NA were excluded for subsequent modeling.

2.2.2. Remote Sensing Image Data

The remote sensing imagery was mainly obtained from the National Aeronautics and Space Administration (NASA) MODIS Level-1B product with a spatial resolution of 1 km and a temporal resolution of 1 day. We downloaded the MODIS Level-1B data from 2016 to 2020. The TOA reflectance values along with the solar zenith/azimuth and satellite zenith/azimuth values that are used to retrieve the AOD values were extracted for modeling.

2.2.3. Meteorological Data

We obtained the meteorological data from NASA's Earth Observing System forward-processed data (GEOS-FP). A total of 10 meteorological variables were extracted in this study (Figure 2).

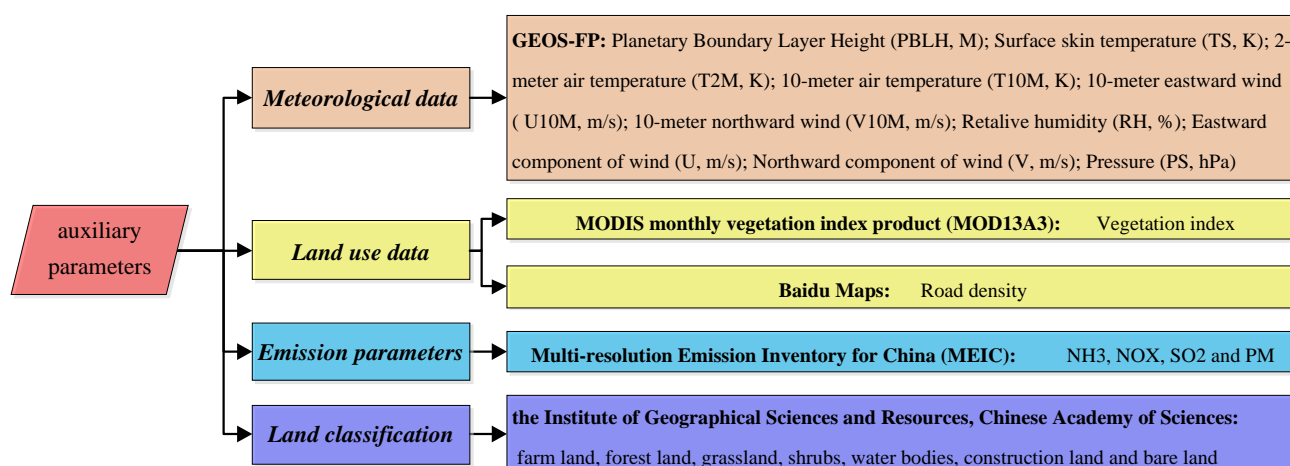


Figure 2. The prescription of the supplemental parameters.

2.2.4. Land Use Data

The vegetation index used for modeling was obtained from the MODIS product (i.e., MOD13A3). Major traffic roads (e.g., highways and national roads) were downloaded from Baidu Maps, and we retrieved the road density by calculating the road vector lengths in each 1×1 km grid for modeling.

2.2.5. Emission Data

The emission parameters including NH_3 , NO_x , SO_2 , and fine particles (PM) from the Multi-resolution Emission Inventory for China (MEIC) were selected in this study. The spatial resolution of emission parameters was $0.25^\circ \times 0.25^\circ$.

2.2.6. Landscape Pattern Index

Three-year land classification imageries (i.e., 2016, 2018, and 2020) with a spatial resolution of 30 m were provided by the Chinese Academy of Sciences (<https://www.resdc.cn/> (accessed on 7 September 2021)). The correlations of county-based average $\text{PM}_{2.5}$ with the land use categories and landscape patterns were investigated. The land classification data defined seven categories over the entire study area. We calculated six landscape pattern indices at a type level, including the proportion of landscape occupied (PLAND), patch density (PD), edge density (ED), the largest class of patches to landscape area proportion (LPI), average patch area (AREA_MN), and shape index (LSI), and seven indices at an overall level, including PD, ED, cohesion (COHES), Landscape Division Index (DIVIS), et al., for each year by using Fragstats 4.2.

All the supplemental parameters used in this study (see Figure 2) were interpolated into 1×1 km plots for data integration; the expressions of all landscape pattern indices are illustrated in Table 1.

2.3. Data Modeling and Validation

Random forest is a machine learning method. It firstly forms a sub-training set by extracting samples from the training set and then generates multiple decision tree models by training the decision trees based on the random feature selection method. Finally, the values of all decision tree predictions are averaged as the output of the random forest. The random forest can handle a large number of input variables, and the training time can be tuned based on a desired accuracy. More importantly, the method can provide the measurement of the prediction strength of each variable, which can yield more interpretable results. For this paper, the MODIS satellite TOA reflectance, 10 meteorological parameters, vegetation index, road density, and four MEIC emissions were used as the input parameters of the random forest model to predict the $\text{PM}_{2.5}$ in the YRD-FJ region. We obtained the optimal model by training two parameters, i.e., the number of predictor variables (mtry)

and the decision trees in each random forest (ntree). The random forest regression model can be simply expressed by the following equation.

$$PM_{2.5} = RF (TOA_{3\text{-bands}}, Zenith_{\text{sun-satellite}}, Azimuth_{\text{sun-satellite}}, Meteoro_{10\text{-parameters}}, Landuse_{2\text{-parameters}}, Emission_{4\text{-parameters}}) \quad (1)$$

where $PM_{2.5}$ is the observed $PM_{2.5}$ concentrations at 195 environmental stations; $TOA_{3\text{-bands}}$ represents the TOA at the blue, red, and mid-infrared bands; $Zenith_{\text{sun-satellite}}$ defines the sun zenith and satellite zenith; $Azimuth_{\text{sun-satellite}}$ includes the sun azimuth and satellite azimuth; $Meteoro_{10\text{-parameters}}$ represents 10 meteorological parameters; $Landuse_{2\text{-parameters}}$ includes two land use parameters; $Emission_{4\text{-parameters}}$ defines four emission parameters; and RF is the random forest model.

Table 1. The expression of landscape pattern index.

Landscape Metrics	Expression	Landscape Metrics	Expression
Percentage of Landscape (PLAND)	$PLAND = \frac{\sum_{i=1}^n a_{ij}}{A} \times 100$	Edge Density (ED)	$ED = \frac{\sum_{i=1}^n e_{ij}}{A} \times 10000$
Patch Density (PD)	$PD = N/A \times 10000 \times 100$	Landscape Shape Index (LSI)	$LSI = \frac{0.25E}{\sqrt{A}}$
Largest Patch Index (LPI)	$LPI = \frac{\max(a_{ij})}{A} \times 100$	Mean Patch Area (AREA_MN)	$AREA_MN = \frac{\sum_{i=1}^n a_{ij}}{N}$
Cohesion (COHES)	$COHES = [1 - \frac{\sum_{j=1}^n p_{ij}}{\sum_{j=1}^n p_{ij} \times \sqrt{a_{ij}}}] [1 - \frac{1}{\sqrt{Z}}]^{-1} \times 100$	Shannon's Diversity Index (SHDI)	$SHDI = - \sum_{i=1}^m [P_i \ln(P_i)]$
Landscape Division Index (DIVIS)	$DIVIS = [1 - \sum_{j=1}^n (\frac{a_{ij}}{A})] \times 100$	Shannon's Evenness Index (SHEI)	$SHEI = \frac{- \sum_{i=1}^m [P_i \ln(P_i)]}{\ln m}$
Aggregation Index (AI)	$AI = [\frac{g_{ii}}{\max \rightarrow g_{ii}}] \times 100$		

Note: a_{ij} represents the area of patch $_{ij}$; A is the total area of landscape; N means the number of the patch; e_{ij} defines the edge length of patch $_{ij}$; E means the total length of all the patch edges; p_{ij} represents the circumference of patch $_{ij}$; Z is the total number of landscape patches; P_i defines the percentage of patch $_i$ to the total patch; g_{ii} represents the number of the similar adjacent patches.

The RF model was validated by using cross validation (CV) with two coefficients, i.e., R^2 and RMSE. The flowchart of this study is presented in Figure 3.

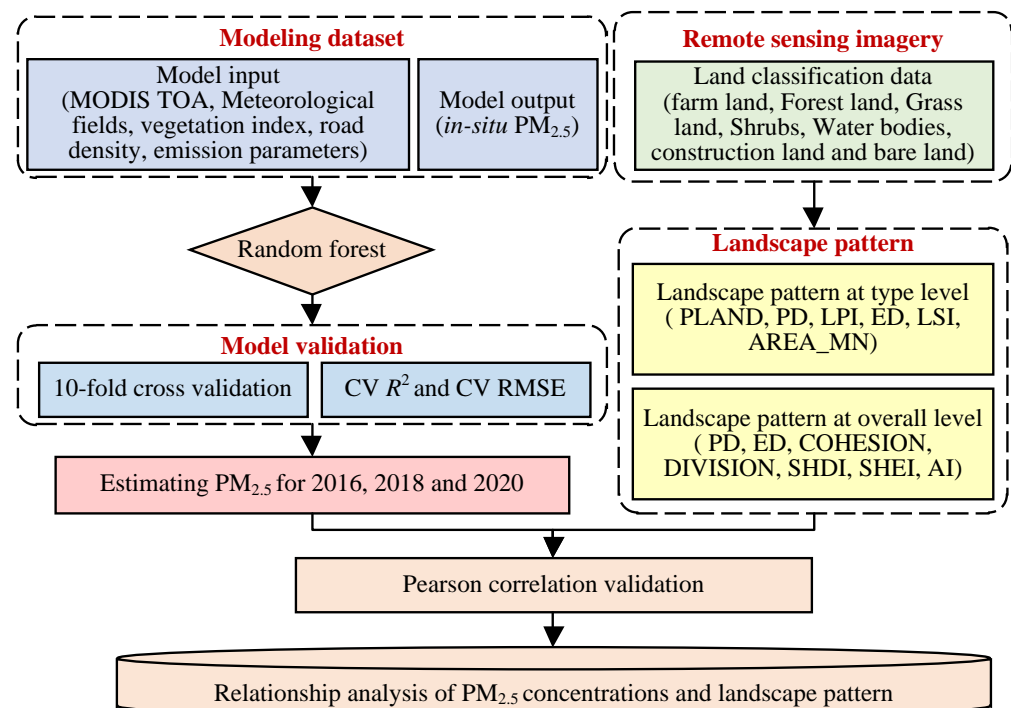


Figure 3. Flowchart of the study.

3. Results and Analysis

3.1. Model Validation and Prediction

The $PM_{2.5}$ concentrations at 195 monitoring stations of the YRD-FJ region showed a decreasing trend with higher $PM_{2.5}$ concentrations in 2016 and much lower values in 2020. From the perspective of regions, Jiangsu and Shanghai, located in the YRD, presented the highest $PM_{2.5}$ values. Zhejiang province exhibited much lower values than Jiangsu, and the lowest $PM_{2.5}$ values were located in Fujian. Figure 4 presents the cross-validation result of the RF model for 3 years in the YRD-FJ region. We achieved a CV R^2 of 0.91 (RMSE = 9.06 $\mu\text{g}/\text{m}^3$), 0.89 (RMSE = 10.19 $\mu\text{g}/\text{m}^3$), and 0.90 (RMSE = 8.02 $\mu\text{g}/\text{m}^3$) in the YRD-FJ region in 2016, 2018, and 2020, respectively.

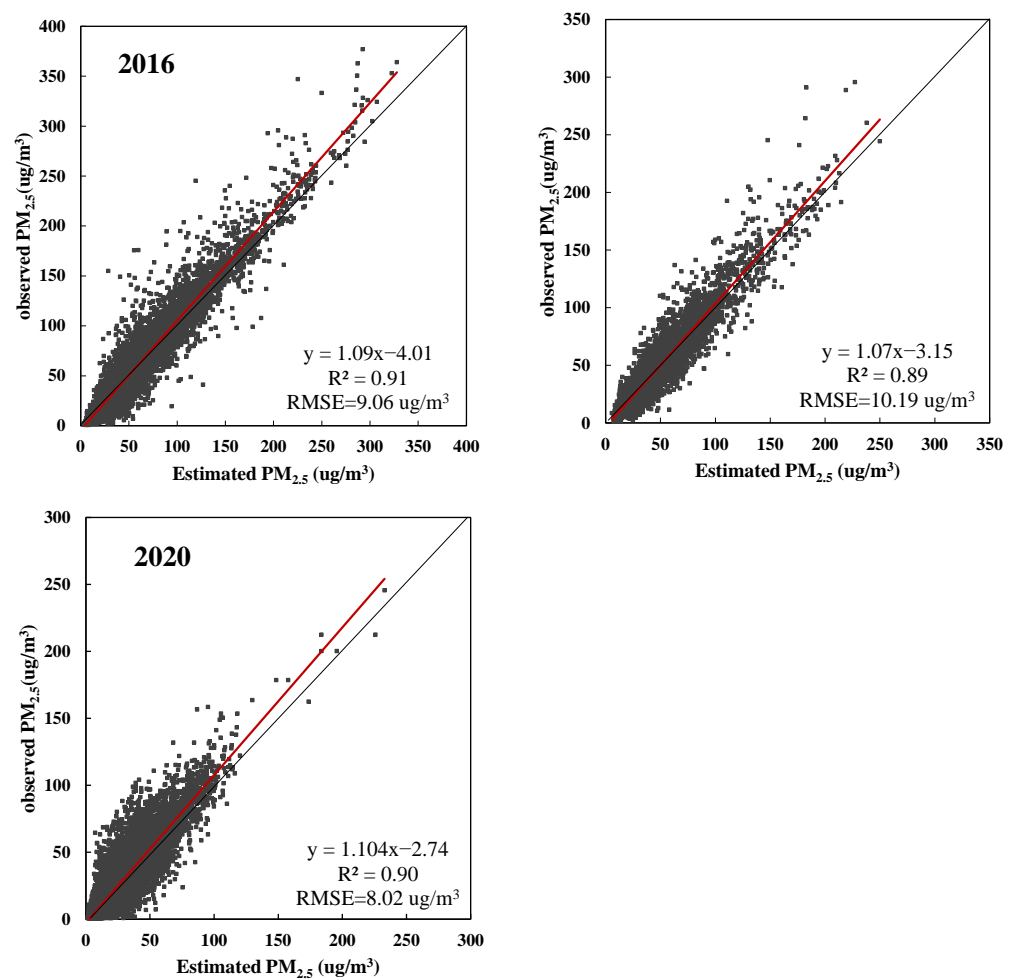


Figure 4. The 10-fold CV validation result of RF model. The red line defines the model-fitting line.

Figure 5 gives the spatial distribution of the $PM_{2.5}$ concentrations retrieved from the RF model in the YRD-FJ region in 2016, 2018, and 2020, respectively. The annual mean $PM_{2.5}$ retrieved from the RF model showed a trend of a year-on-year decrease, with much higher values in 2016 and lower values in 2020. From the perspective of four individual regions, there was an obvious $PM_{2.5}$ distribution pattern of “Jiangsu > Shanghai > Zhejiang > Fujian” for 3 years in the YRD-FJ region, which was consistent with that from the monitoring stations. The annual mean $PM_{2.5}$ concentrations reached the highest values of 57.32, 49.22, 38.19, and 28.30 $\mu\text{g}/\text{m}^3$ in Jiangsu, Shanghai, Zhejiang, and Fujian, respectively, in 2016. This may be closely related to the distribution of land cover and local industries accompanied by increasing human activities; the use of resources and energy brought by urban industrialization has largely affected the air quality. The annual mean $PM_{2.5}$ concentrations showed the lowest values of 37.67, 28.54, 23.48, and 19.87 $\mu\text{g}/\text{m}^3$ in Jiangsu,

Shanghai, Zhejiang, and Fujian in 2018, respectively, with a decrease of 19.65, 20.68, 14.71, and 8.42 $\mu\text{g}/\text{m}^3$ compared with those in 2016. This was largely due to the reduction in human activities caused by the COVID-19 pandemic.

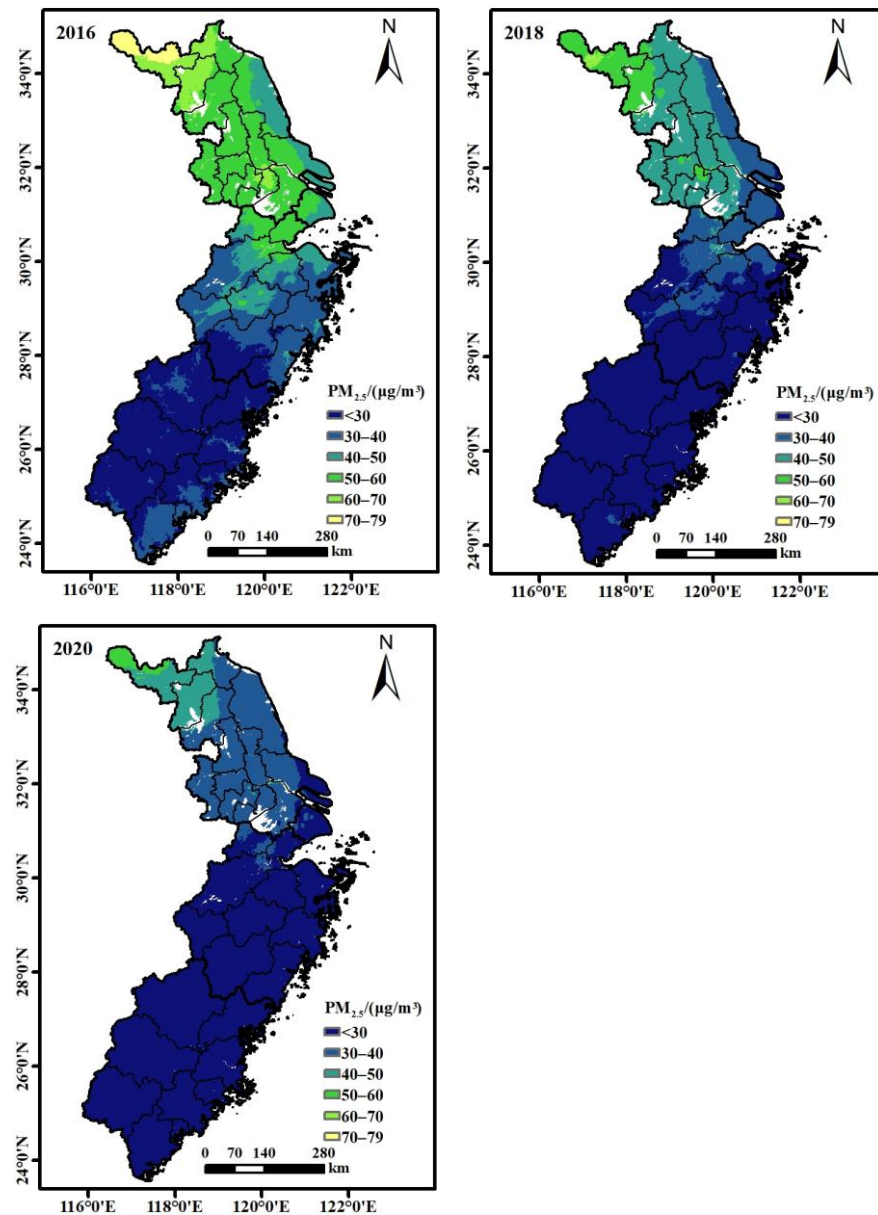


Figure 5. The $\text{PM}_{2.5}$ distribution of the YRD-FJ region from 2016 to 2020.

At city scale, most of the cities witnessed the highest $\text{PM}_{2.5}$ concentrations in Jiangsu province ($31\text{--}70\ \mu\text{g}/\text{m}^3$), where Xuzhou was the most air polluted city with 3-year average $\text{PM}_{2.5}$ concentrations higher than $51\ \mu\text{g}/\text{m}^3$. The $\text{PM}_{2.5}$ concentrations of all cities were relatively low ($19\text{--}31\ \mu\text{g}/\text{m}^3$) in Fujian province. The highest value was located in Xiamen, with 3-year average $\text{PM}_{2.5}$ values of $26\ \mu\text{g}/\text{m}^3$, which was also much lower than those of cities in other provinces. At county scale, the 10 counties with the highest $\text{PM}_{2.5}$ concentrations were Pei, Feng, Jiawang, Pizhou, Quanshan, Tongshan, Yunlong, Suining, Xinyi, and Suyu, which are all located in Jiangsu Province. The lowest $\text{PM}_{2.5}$ concentrations were located in seven counties of Fujian Province (i.e., Gutian, Zherong, Zhenghe, Dehua, Shouning, Pingnan, and Zhouning) and two counties of Zhejiang Province (i.e., Qingyuan and Taishun).

3.2. Relationship between PM_{2.5} and Landscape Pattern at Type Level

We calculated the correlation of county-based PM_{2.5} values and the landscape pattern indices at type level by using the Pearson coefficient in the YRD and Fujian region in 2016, 2018, and 2020, respectively. Figure 6 gives the result of the relationship between PM_{2.5} concentrations and landscape pattern at type level. Overall, the county-based annual mean PM_{2.5} presented a highly significant correlation with four landscape types, i.e., forest land, farmland, water bodies, and construction land, while three types (i.e., shrub, grass, and bare land) were not strongly associated with the PM_{2.5} values. Except for forest land, most of the type level indices of farmland, water bodies, and construction land were positively related with PM_{2.5} concentrations.

As for farmland, PLAND, LPI, and ED presented a significant correlation with the county-based PM_{2.5} concentrations ($r \sim 0.74$). The larger PLAND, LPI, and ED led to higher average PM_{2.5} concentrations, and the smoke caused by straw burning after a harvest was also responsible for the higher annual mean PM_{2.5} concentrations. The PLAND, PD, LPI, and ED of the construction land also showed a positive correlation with the county-based PM_{2.5} concentrations ($r \sim 0.71$), where the PLAND–PM_{2.5} relationship was the highest of all. With rapid urbanization, the higher proportion of the largest patches of built-up landscapes to the landscape area and the higher edge density increased the annual mean PM_{2.5} concentrations. Therefore, it is necessary to reasonably control edge areas and reduce the degree of fragmentation in urban expansion. The correlation of PM_{2.5} and AREA_MN of water bodies was relatively low; the larger PLAND, LPI, ED, and AREA-MN made the PM_{2.5} concentrations much higher. This is possibly because most of the buildings are distributed around water bodies (i.e., an important supply for human lives), and the PM_{2.5} concentrations might seriously be affected by the high buildings and human activities.

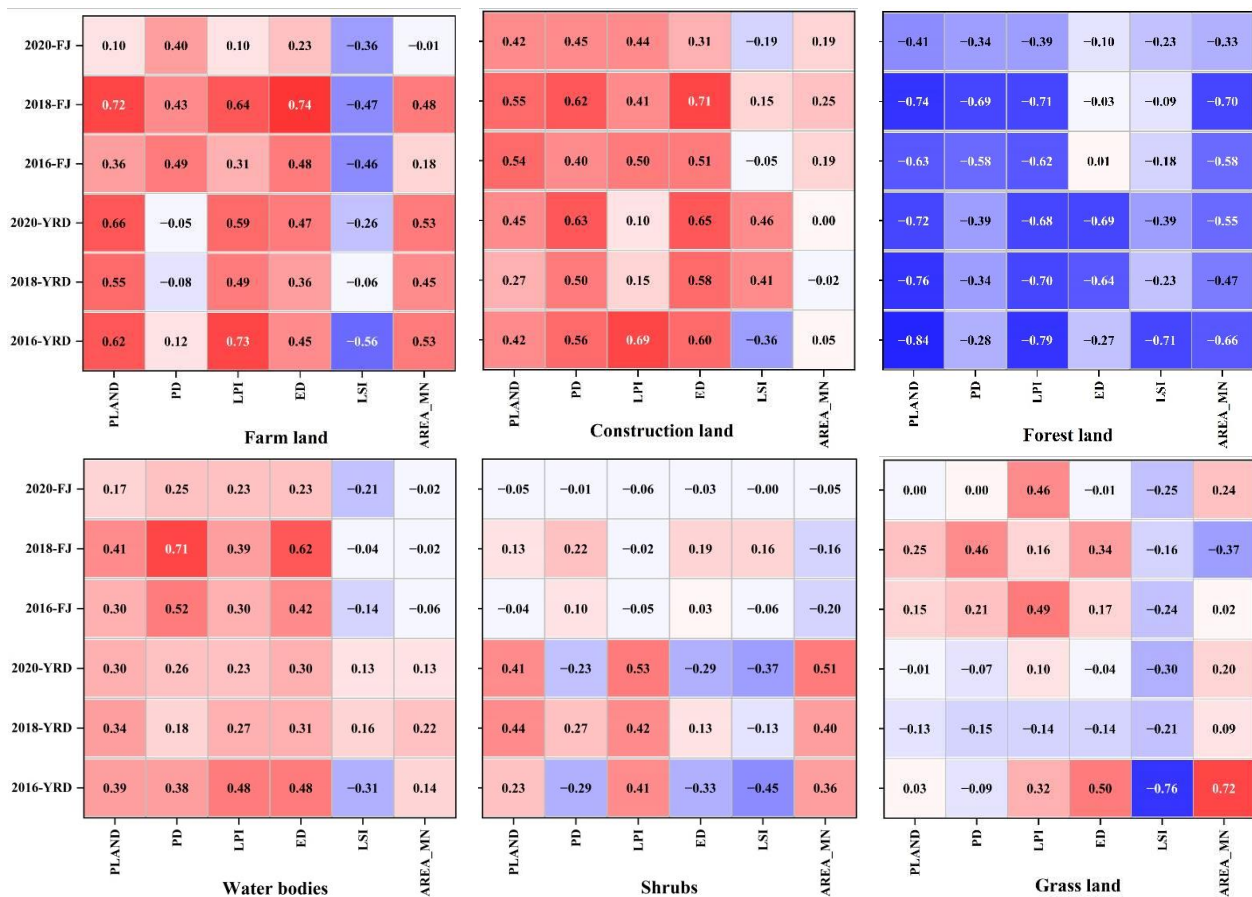


Figure 6. Cont.

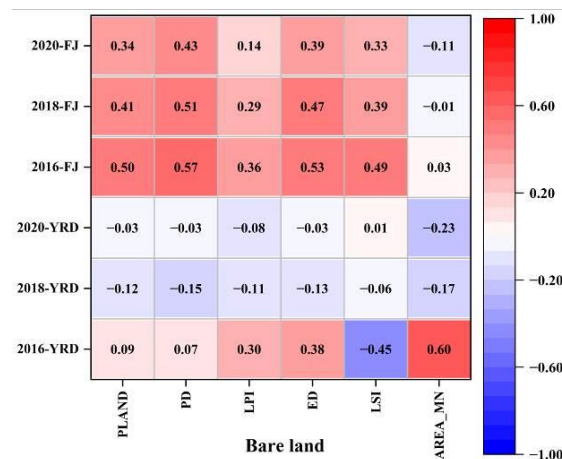


Figure 6. Correlation coefficients between six landscape patterns and $PM_{2.5}$.

For the forest land, most of the indices were significantly correlated with county-based annual mean $PM_{2.5}$ concentrations ($r \sim 0.84$), where PLAND, LPI, and AREA-MN showed a much higher correlation than LSI and ED, indicating that the proportion of landscapes, the dominance, and fragmentation had a more significant effect on reducing $PM_{2.5}$ concentrations than the landscape shape and structural features. On the other hand, forest land adsorbs an aerosol through the dry and wet depositions of leaves to reduce the surrounding $PM_{2.5}$ concentrations, which has a significant effect on the reduction in atmospheric particulate matter and the improvement of air quality.

3.3. Relationship between Overall Landscape Pattern and $PM_{2.5}$

Seven landscape pattern indices including PD, ED, COHES, DIVIS, SHDI, SHEI, and AI were calculated; only COHES and AI were significantly negatively related with $PM_{2.5}$ concentrations ($r \sim 0.80$) (Figure 7). COHES and AI represented the connectivity and aggregation of the landscape, respectively, indicating that enhancing the patchiness and aggregation of forest land could effectively alleviate the fragmentation of the landscape and, thus, could improve the dust retention effect on the annual mean $PM_{2.5}$ concentrations. Three indices, i.e., PD, ED, and SHEI, which reflect the degree of fragmentation of all types of landscapes in the region, were positively related with $PM_{2.5}$ concentrations. It can be concluded that the forest land with high fragmentation would lead to high $PM_{2.5}$ pollution due to the dust retention effect of the fragmented landscape. DIVIS and SHDI showed relatively low correlation with $PM_{2.5}$ concentrations.

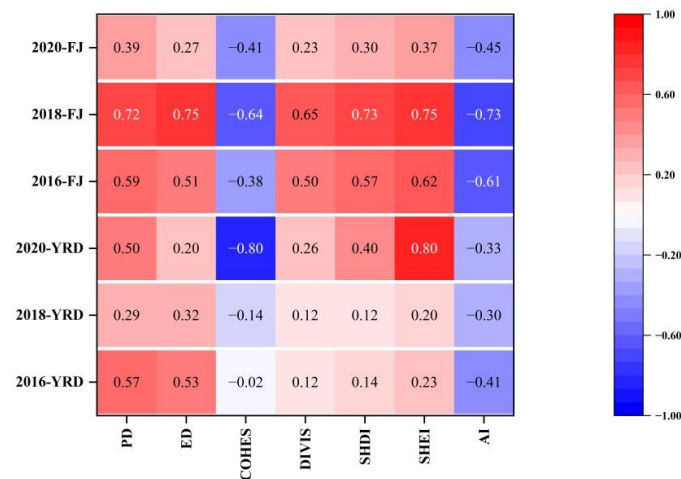


Figure 7. Correlation coefficients between annual mean $PM_{2.5}$ concentrations and landscape pattern index at overall level.

4. Discussion

The YRD-FJ region is an important part of the coastal economic belt as well as the ecological barrier area in China. Previous studies mainly focused on urban agglomerations with poor air quality, such as Sichuan Basin, the YRD, etc., while no study has been reported using the contiguous region of the YRD (the region with poor air quality) and FJ (the region with good air quality) as the study area. The advantages of using the YRD-FJ region as the study area are mainly: (1) the modeling data set with a wider dynamic range provided by the contiguous area would make the model more stable and explainable than that of a single region and (2) although both of these two regions are located in the coastal region of China, their topographies are totally different, i.e., the YRD region is dominated by plains, while an area of mountains and hills reaches up to 80% in Fujian Province. Therefore, our results could provide a more scientific basis and support due to the large topographic differences of these two regions.

In this paper, we used a total of 10 meteorological variables, two land use parameters, and four emission indices to establish the RF model. At the beginning of the model's construction, we tried to apply 18 meteorological variables for PM_{2.5} prediction; however, the model's predictability could not be proven by adding some variables that showed a low correlation with PM_{2.5} (e.g., sea level pressure, vertical pressure velocity, etc.). The vegetation index and road density were employed to represent the forest coverage and vehicle emission, respectively, which are closely related with PM_{2.5} pollution. We also calculated the relationship of other emission parameters, such as CO and PM_{2.5} concentrations, and the results showed that their correlation was extremely low ($r = 0.01$). Overall, the PM_{2.5} concentrations presented a generally descending trend from 2016 to 2020, indicating that the construction of an ecological civilization during the last decade has effectively improved the air quality in the YRD region. The results derived from the RF model using remote sensing imageries and other auxiliary variables were consistent with previous studies, which all showed a pattern of Jiangsu > Shanghai > Zhejiang > Fujian.

Thus far, studies on the correlation of landscape patterns and PM_{2.5} mainly used the in situ data from environmental monitoring stations in small- and medium-scale areas. They established the buffer zones with various radiuses centered on the monitoring stations to explore their relationships. This buffer zone-based method could reflect the real situation of a landscape pattern more accurately, but it is hard to choose the optimal radius for the buffer zone. Previous studies also retrieved the landscape pattern index by using the whole administrative area as a single unit or by using the element-by-element (moving window) method. Both of these two methods have certain limitations, e.g., taking the whole administrative area as a single unit would make it difficult to explore the changes of landscape pattern at fine scales while the element-by-element (moving window) approach cannot easily obtain the optimal moving window scale for the study area. For example, we revealed that the landscape pattern indices calculated by using moving the window method were not significantly correlated with PM_{2.5} concentrations ($r = 0.01\sim 0.1$) in southwest China. In this study, there were 285 districts/counties in the YRD-FJ region, most of which exhibited much higher PM_{2.5} concentrations in Jiangsu province than those in Fujian Province. Therefore, our research focusing on the landscape patterns and PM_{2.5} concentrations based on 285 districts/counties with different air pollution levels avoided the limitations of those two abovementioned methods.

In this study, we not only investigated the impact of land types that have significant effects on PM_{2.5} concentrations, such as forest land, construction land, and water bodies, on air quality, but also discussed the effect of other landscape patterns such as shrubs, grass land, and bare land on the annual mean PM_{2.5} concentrations in the study area. It can be concluded that the proportions of maximum patches to landscape area (LPI), edge density (ED), shape index (LSI), and mean patch area (AREA-MN) of shrubs, grass land, and bare land were related to the PM_{2.5} in the YRD. The indices of shrubs did not show satisfactory correlations with PM_{2.5} concentrations in Fujian. At an overall level, all types of indices exhibited varying degrees of correlation with county-based annual mean

PM_{2.5} concentrations. We also tried to understand the relationship between PM_{2.5} values and landscape pattern by using buffer zones with different radiuses centered on ground monitoring stations as well as the moving window method; the results showed rather weak correlations between landscape pattern indices and annual mean PM_{2.5} concentrations. Our results can provide a scientific support of how to integrate the landscape ecology into air pollution management for an ecological department. However, there were also some limitations in this study. For example, whether the landscape pattern could affect the seasonal PM_{2.5} was not explored. Second, although the landscape pattern was highly correlated with PM_{2.5} concentrations, there was a time lag for the landscape pattern and the real-time PM_{2.5} change. In addition to the local climate, topography, and landscape pattern, the inter-regional transmission of the atmospheric pollutants also affects the PM_{2.5} concentrations in FJ province as the PM_{2.5} of the YRD region was much higher than that of FJ province. Therefore, future studies will focus on the effects of seasonal differences and inter-regional transmission on regional PM_{2.5} concentrations.

5. Conclusions

In this paper, we validated the predictability of the RF model using MODIS TOA reflectance and four categories of supplemental variables in estimating the PM_{2.5} concentrations in the region of the YRD-FJ. Satisfactory results with R^2 of 0.91, 0.89, and 0.90 in 2016, 2018, and 2020, respectively, were obtained, which outperformed most of the previous studies. The PM_{2.5} concentrations and their correlations with landscape indices at two levels were also discussed. In addition to the land types that had significant effects on PM_{2.5} concentrations (i.e., forest land, construction land, and water bodies), the landscape pattern indices of shrubs, grass land, and bare land (e.g., LPI, ED, and AREA-MN) were also related to the PM_{2.5} values. The county-based annual mean PM_{2.5} presented a highly significant correlation with four landscape types, i.e., forest land, farmland, water bodies, and construction land, while three types (i.e., shrub, grass, and bare land) were not strongly associated with the PM_{2.5} values. Moreover, three indices, i.e., PD, ED, and SHEI, which reflect the degree of fragmentation of all types of landscapes in the region, were positively related with PM_{2.5} concentrations. The results suggest that reasonable control of land use and the effective landscape layout of different land use types would improve the air quality of the YRD-FJ region.

Author Contributions: Conceptualization, L.Y. and T.S.; methodology, L.Y.; software, L.Y. and S.W.; validation, X.H.; formal analysis, L.Y. and X.H.; investigation, X.H. and S.W.; resources, S.W. and X.H.; data curation, L.Y. and S.W.; writing—original draft preparation, L.Y.; writing—review and editing, T.S.; visualization, S.W.; supervision, T.S.; project administration, S.W.; funding acquisition, L.Y. and T.S. All authors have read and agreed to the published version of the manuscript.

Funding: This work was supported by the Science and Technology Department of Fujian Province (Nos. 2021R0123 and 2022J05244), Minjiang University (Nos. MJY20001 and MJY21018), Fujian Educational Bureau (Nos. 2021JAT200435 and JAT200423), and Fujian Social Science Foundation Project (FJ2021C090).

Institutional Review Board Statement: Not applicable.

Informed Consent Statement: Not applicable.

Data Availability Statement: The dataset on which this paper is based is too large to be retained or publicly archived with available resources. Documentation and methods used to support this study are available from the first author (Email: 2611@mju.edu.cn) at Minjiang University.

Acknowledgments: The authors would like to thank NASA for the use of MODIS and GEOS-FP data.

Conflicts of Interest: The authors declare no conflict of interest.

References

1. Peng, L.; Shen, Y.L.; Gao, W.; Zhou, J.; Pan, L.; Kan, H.D.; Cai, J. Personal exposure to PM_{2.5} in five commuting modes under hazy and non-hazy conditions. *Environ. Pollut.* **2021**, *289*, 117823. [[CrossRef](#)]
2. Dong, G.-H. Ambient air pollution in China. *Respirology* **2019**, *24*, 626–627. [[CrossRef](#)]
3. Yang, L.; Xing, Y.; Jones, P. Exploring the potential for air pollution mitigation by urban green infrastructure for high density urban environment. In Proceedings of the 3rd International Conference on Energy Engineering and Environmental Protection (EEEP), Sanya, China, 19–21 November 2019.
4. Rojas-Rueda, D.; Vrijheid, M.; Robinson, O.; Marit, A.G.; Grazuleviciene, R.; Slama, R.; Nieuwenhuijsen, M. Environmental Burden of Childhood Disease in Europe. *J. Environ. Res. Public Health* **2019**, *16*, 1084. [[CrossRef](#)]
5. Wang, Z.T.; Gao, S.L.; Xie, J.F.; Li, R.J. Identification of multiple dysregulated metabolic pathways by GC-MS-based profiling of lung tissue in mice with PM_{2.5}-induced asthma. *Chemosphere* **2019**, *220*, 1–10. [[CrossRef](#)] [[PubMed](#)]
6. Hu, X.F.; Waller, L.A.; Al-Hamdan, M.Z.; Crosson, W.L.; Estes, M.G.; Estes, S.M.; Quattrochi, D.A.; Sarnat, J.A.; Liu, Y. Estimating ground-level PM_{2.5} concentrations in the southeastern US using geographically weighted regression. *Environ. Res.* **2013**, *121*, 1–10. [[CrossRef](#)] [[PubMed](#)]
7. Matci, D.K.; Kaplan, G.; Avdan, U. Changes in air quality over different land covers associated with COVID-19 in Turkey aided by GEE. *Environ. Monit. Assess.* **2022**, *194*, 762. [[CrossRef](#)] [[PubMed](#)]
8. Gladson, L.; Garcia, N.; Bi, J.; Liu, Y.; Lee, H.J.; Cromar, K. Evaluating the Utility of High-Resolution Spatiotemporal Air Pollution Data in Estimating Local PM_{2.5} Exposures in California from 2015–2018. *Atmosphere* **2022**, *13*, 85. [[CrossRef](#)]
9. Pan, S.; Du, S.S.; Wang, X.R.; Zhang, X.X.; Xia, L.; Liu, J.P.; Pei, F.; Wei, Y.X. Analysis and interpretation of the particulate matter (PM₁₀ and PM_{2.5}) concentrations at the subway stations in Beijing, China. *Sustain. Cities Soc.* **2019**, *45*, 366–377. [[CrossRef](#)]
10. Wang, Y.Y.; Shi, Z.H.; Shen, F.Z.; Sun, J.J.; Huang, L.; Zhang, H.L.; Chen, C.; Li, T.T.; Hu, J.L. Associations of daily mortality with short-term exposure to PM_{2.5} and its constituents in Shanghai, China. *Chemosphere* **2019**, *233*, 879–887. [[CrossRef](#)]
11. Liu, Y.; Sarnat, J.A.; Kilaru, A.; Jacob, D.J.; Koutrakis, P. Estimating ground-level PM_{2.5} in the eastern united states using satellite remote sensing. *Environ. Sci. Technol.* **2005**, *39*, 3269–3278. [[CrossRef](#)]
12. Michanowicz, D.R.; Shmool, J.L.C.; Tunno, B.J.; Tripathy, S.; Gillooly, S.; Kinnee, E.; Clougherty, J.E. A hybrid land use regression/AERMOD model for predicting intra-urban variation in PM_{2.5}. *Atmos. Environ.* **2016**, *131*, 307–315. [[CrossRef](#)]
13. Mehdipour, V.; Stevenson, D.S.; Memarianfard, M.; Sihag, P. Comparing different methods for statistical modeling of particulate matter in Tehran, Iran. *Air Qual. Atmos. Health* **2018**, *11*, 1155–1165. [[CrossRef](#)]
14. Brokamp, C.; Jandarov, R.; Hossain, M.; Ryan, P. Predicting Daily Urban Fine Particulate Matter Concentrations Using a Random Forest Model. *Environ. Sci. Technol.* **2018**, *52*, 4173–4179. [[CrossRef](#)] [[PubMed](#)]
15. Vu, B.N.; Sanchez, O.; Bi, J.Z.; Xiao, Q.Y.; Hansel, N.N.; Checkley, W.; Gonzales, G.F.; Steenland, K.; Liu, Y. Developing an Advanced PM_{2.5} Exposure Model in Lima, Peru. *Remote Sens.* **2019**, *11*, 641. [[CrossRef](#)] [[PubMed](#)]
16. Ma, Z.W.; Liu, Y.; Zhao, Q.Y.; Liu, M.M.; Zhou, Y.C.; Bi, J. Satellite-derived high resolution PM_{2.5} concentrations in Yangtze River Delta Region of China using improved linear mixed effects model. *Atmos. Environ.* **2016**, *133*, 156–164. [[CrossRef](#)]
17. He, Q.Q.; Huang, B. Satellite-based mapping of daily high-resolution ground PM_{2.5} in China via space-time regression modeling. *Remote Sens. Environ.* **2018**, *206*, 72–83. [[CrossRef](#)]
18. Yang, L.; Shi, T.; Lin, M.; Wu, J.; Wang, S.; Liu, Y. Development of the TOA-Related Models for PM_{2.5} Prediction Pre- and Post-COVID-19 Outbreak over Yangtze River Delta Region of China. *J. Sens.* **2022**, *2022*, 2994885. [[CrossRef](#)]
19. Zhang, L.; Hao, J.; Xu, W. PM_{2.5} and PM₁₀ Concentration Estimation Based on the Top-of-Atmosphere Reflectance. In Proceedings of the 16th International Conference on Wireless Algorithms, Systems, and Applications (WASA), Nanjing, China, 25–27 June 2021; pp. 574–581.
20. Zhong, X.; Zhao, Y.; Sha, J.; Liang, H.; Wu, P. Spatiotemporal variations of air pollution and population exposure in Shandong Province, eastern China, 2014–2018. *Environ. Monit. Assess.* **2022**, *194*, 114. [[CrossRef](#)] [[PubMed](#)]
21. Jin, H.; Zhong, R.; Liu, M.; Ye, C.; Chen, X. Spatiotemporal distribution characteristics of PM_{2.5} concentration in China from 2000 to 2018 and its impact on population. *J. Environ. Manag.* **2022**, *323*, 116273. [[CrossRef](#)] [[PubMed](#)]
22. McCarty, J.; Kaza, N. Urban form and air quality in the United States. *Landscape Urban Plan.* **2015**, *139*, 168–179. [[CrossRef](#)]
23. Huang, C.-S.; Liao, H.-T.; Lu, S.-H.; Chan, C.-C.; Wu, C.-F. Identifying and quantifying PM_{2.5} pollution episodes with a fusion method of moving window technique and constrained Positive Matrix Factorization. *Environ. Pollut.* **2022**, *315*, 120382. [[CrossRef](#)] [[PubMed](#)]
24. Crouse, D.L.; Erickson, A.C.; Christidis, T.; Pinault, L.; van Donkelaar, A.; Li, C.; Meng, J.; Martin, R.V.; Tjepkema, M.; Hystad, P.; et al. Evaluating the Sensitivity of PM_{2.5}-Mortality Associations to the Spatial and Temporal Scale of Exposure Assessment. *Epidemiology* **2020**, *31*, 168–176. [[CrossRef](#)] [[PubMed](#)]

Disclaimer/Publisher’s Note: The statements, opinions and data contained in all publications are solely those of the individual author(s) and contributor(s) and not of MDPI and/or the editor(s). MDPI and/or the editor(s) disclaim responsibility for any injury to people or property resulting from any ideas, methods, instructions or products referred to in the content.